ELSEVIER

Catalysis Today 49 (1999) 277–284

CATALYSIS TODAY

Characterization of metal-incorporated molecular sieves

K.J. Chao[a,*], A.C. Wei[a], H.C. Wu[a], J.F. Lee[b]

[a]Department of Chemistry, National Tsing Hua University, Hsinchu 300, Taiwan
[b]Synchrotron Radiation Research Center, Hsinchu 300, Taiwan

Abstract

Metal-containing aluminophosphate molecular sieves (MeAPOs) were observed to exhibit remarkable catalytic activity in partial oxidation of hydrocarbons under mild condition. In this paper we review the spectroscopic characterization of framework incorporation and redox behavior of vanadium and cobalt in MeAPOs. EXAFS/XANES and XPS studies of the oxidation state and coordination of V and Co in as-prepared MeAPOs and after redox treatments will also be presented. These studies show that fourfold coordinated Co^{2+} of CoAPO-11 was only partially oxidized to Co^{3+}, while grafted V^{4+} of VAPO-5 was almost completely oxidized to V^{5+} after calcination. All Co and V species remain in the $AlPO_4$ framework during redox treatments. © 1999 Elsevier Science B.V. All rights reserved.

Keywords: Molecular sieves; Metal-containing aluminophosphate

1. Introduction

Because of their effect on acid and redox behaviors of zeolite-type catalysts, the metal incorporation in silicate, aluminosilicate and aluminophosphate molecular sieves have received wide attention [1–3]. Metals may stay in the tetrahedral framework or the intraframework cavities of MeAPOs as metal oxides or counter ions. The understanding of extraframework metal species has been well established and the framework metal species were recently found to be responsible for some unique catalytic properties which are very much dependent on their encapsulation in zeolitic framework, i.e. titanium in TS-1 [3,4]. Besides the modification of acidity, the presence of multivalent transition metal cations in the framework can also create isolated redox centers. If the metal cation replaces one of the T-atoms in the regular tetrahedral framework, it should be in a fourfold coordination. During oxidation reactions, reactants and sometime solvents are required to enter the framework cavities and attach themselves to the framework metal sites resulting in some changes in the coordination state of metal cations, which, in turn, may involve non-tetrahedral coordination and ligand exchange. As for the redox behavior of metal cations, we may consider framework metal species as the one which has been separately incorporated in the framework and were bound to framework TO_4 units through oxygen atoms or were grafted on the internal surface of zeolites through condensation with two or more terminal zeolitic O–H groups.

Comparing with silicate and aluminosilicate, aluminophosphate framework was considered to be flexible enough to accommodate low levels of other ions [1,5]. Among a large number of metal ions, cobalt and vanadium were considered to be capable of incorporating in $AlPO_4$ framework and their catalytic activity on oxidation reactions were confirmed by various

---

*Corresponding author. Fax: +886-3-5720964; e-mail: kjchao@chem.nthu.edu.tw

0920-5861/99/$ – see front matter © 1999 Elsevier Science B.V. All rights reserved.
PII: S0920-5861(98)00434-9

structural analyses and catalytic testing studies [6–10]. In this paper, we will focus on the spectroscopic characterization of the chemical features of framework cobalt and vanadium species in MeAPO molecular sieves during redox treatments. This information should be of great usefulness for the preparation of metal-incorporated zeolite-type materials, and for applications in catalytic oxidation.

2. CoAPO molecular sieves

2.1. Isomorphous substitution

Co^{2+} substitution in $AlPO_4$ were confirmed to occur exclusively on Al tetrahedral sites by both structural and compositional analyses [2,6,8,11–14] and X-ray diffraction is one of the key structural techniques used. Single crystal data show that the amount of Co substitution for Al can be estimated by the refinement of occupancy factors due to the significant difference between X-ray scattering factors of Co and Al [9,10]. Since the T–O length of Al^{3+}–O=0.17 nm and that of Co^{2+}–O=0.19 nm, the average bond length (Me–O) for Co/Al sites in Co-contained zeolite of well-refined structures was expected to increase linearly with the Co/Al ratio [14]. However, unlike Al in aluminosilicate FAU zeolites and Ga in galosilicate β zeolites [2], the cell volumes seem to remain relatively constant in as-prepared CoAPO-5 materials [9]. This may be explained by the distortion of framework derived from the partial occupancy of some tetrahedral sites by Co. When the content of metal (here Co) substitution is high or the metal cations occupation is concentrated at some specific sites, X-ray diffraction structural analysis can provide a reasonable information about the local bonding nature of framework Co. However, this is, in general, not the case for CoAPOs.

For understanding the local structure of active sites, like Co ions, X-ray absorption (XAS) including pre-edge and near-edge spectra (XANES), combined with extended fine structure analysis (EXAFS), is an ideal tool. EXAFS/XANES can provide bonding parameters of Co with adjacent O atoms and the average oxidation states of cobalt cations. The Co species in as-prepared CoAPOs were observed by XAS to exist in four coordination states with the dominated Co–O bond length of 1.92–1.95 Å in CoAPO-5, -18, -36 and -44 [15]. These Co species could stay in the framework after redox treatment as shown in Table 1.

Since the d–d electronic transition for $^4A_2 \rightarrow {}^4T_1(P)$ of Co^{2+} in tetrahedral system presents a com-

Table 1
Structural parameters[a] of CoAPO

Samples		R (Å)	N	σ^2
CoAPO-11[a]				
As-prepared	Co–O	1.95	4	5.2×10^{-3}
Calcined	Co–O_1	1.90	1.0	6.2×10^{-3}
	Co–O_2	2.00	2.5	6.2×10^{-3}
Reduced	Co–O_1	1.96	0.9	8.5×10^{-3}
	Co–O_2	2.03	2.6	8.5×10^{-3}
CoAPO-5[b]				
As-prepared	Co–O	1.94	3.9	3.7×10^{-3}
Calcined	Co–O	1.92	3.6	9×10^{-3}
Reduced	Co–O	1.94	3.9	8.5×10^{-3}
CoAPO-18[b]				
As-prepared	Co–O	1.93	3.8	3.5×10^{-3}
Calcined	Co–O_1	1.82	3.0	3×10^{-3}
	Co–O_2	2.04	1.0	7×10^{-3}
Reduced	Co–O_1	1.90	3.0	4×10^{-3}
	Co–O_2	2.04	1.0	7.5×10^{-3}

[a] R: bond distance, N: coordination number, σ^2: Debye–Waller factor.
[b] [15].

posite profile at 500–650 nm and with stronger absorbance in UV–Vis spectra [16], all as-prepared CoAPOs exhibit blue color. Although the electron absorption spectra lack structural sensitivity, their integrated absorption intensity could still be employed to estimate the amount of Co^{2+} species in a high spin (d^7) state which, in turn, presents itself as a broad paramagnetic signal with $g_\perp=1.9$ and $g_\parallel=4.4$ in the EPR spectra [6,13].

The incorporation of paramagnetic Co ions into an aluminophosphate framework resolves in a decrease in the spin-relaxation time T_1 of the framework ^{31}P nuclei as shown by NMR spectroscopy [17,18]. The effect is dependent on the distance between Co and P in the framework. If Brønsted acidity could be generated by isomorphous substitution of Co^{2+} for Al^{3+}, the OH band in IR and TPD of NH_3 method would be useful to confirm the incorporation of Co^{2+} into the zeolitic framework as well as to monitor acidity. Two different types of acid sites were detected on CoAPO-11 by TPD of NH_3 [19]. Three desorption peaks could be observed on NH_3 adsorbed on template-free CoAPO-5, the lower temperature one at ca. 190°C is ascribable to physically adsorbed NH_3 as suggested by Niwa et al. [20], while the change in enthalpy upon adsorption and the number and the strength of the acid sites ($\Delta H=131$ kJ/mol, 0.38 mmol/g close to 80% of Co content for $T_d\cong320°C$, $\Delta H=200$ kJ/mol, 0.05 mmol/g for $T_d=500°C$) are derived from the higher temperature peaks. The amounts of acid sites ($T_d=320$–370°C) of similar strength on calcined and reduced CoAPO-5 are found to be 0.24 and 0.32 mmol/g, respectively. Furthermore, IR measurements of oxidized and reduced CoAPO-5 show considerable intensity of ν OH at 3661 and 3665 cm^{-1}. However, upon combining either with pyridine or acetonitrile adsorption, IR showed that CoAPO-5 and CoAPO-11 exhibited mainly Lewis acid sites rather than the generally expected Brønsted acid sites as reported by Peeters [21], while reduced CoAPO-18 could provide Brønsted acid sites to give a (Co)–OH–(P) band at 3573 cm^{-1} with (P)–OH band at 3678 cm^{-1} as suggested by Thomas et al. [22].

2.2. *Redox behavior*

Both CoAPO–5 and CoAPO–11 were found to be active and selective for the autoxidation of *p*-cresol to *p*-hydroxy benzaldehyde in methanol/sodium hydroxide solution [23], while CoAPO-5 was observed to be active in the oxidation of cyclohexane and *n*-hexane in the presence of acetic acid or acetone under O_2 [8,24] and in the oxidative dehydrogenation of ethane under oxygen [24]. CoAPO-11 was shown to be active in the liquid phase hydroxylation of phenol to hydroquinone using hydrogen peroxide [25]. These findings suggest that CoAPO-5 and -11 are potential catalysts for selective oxidation.

The proposed reaction mechanism for the oxidation could be either a reversible one-electron transfer, involving the formation of free radicals with redox between Co^{3+} and Co^{2+} [8], or a process begins with free radical autoxidation of hydrocarbons and followed by selectively catalyzed intramolecular heterolytic decomposition of the cyclohexyl hydroperoxide intermediate [26]. The existence of Co^{3+} and Co^{2+} in calcined and reduced CoAPO-5 materials was proposed based on the results from electron absorption spectroscopy [21] and EPR [8,13]. The reduced and as-prepared CoAPO-5 exhibit blue color with a broad paramagnetic EPR signal whereas the calcined materials exhibit green color for CoAPO-5 and yellow green color for CoAPO-11 with no EPR signal. However, the O_2-calcined green CoAPO-5 was also found to return directly to blue color either by evacuation at elevated temperature as shown by us and Chen et al. [27] or through exposure to methanol vapor at room temperature [12]. Kevan and Gorte and others [28] suggested an alternative explanation that calcination and O_2 adsorption might have brought distortion of the coordination sphere around Co^{2+} rather than the oxidation of Co^{2+} to Co^{3+}. EXAFS/XANES results indicated that only ~20% of framework Co^{2+} was oxidized and most of the rest in CoAPO-5 remained in the unoxidized state after calcination, while the complete oxidation of Co^{2+} to Co^{3+} has only occurred in calcined CoAPO-18 as reported by Sankar and Catlow and others [15]. They also suggested that calcination treatment could produce one oxygen vacancy for every two unoxidized Co^{2+} species through severe dehydroxylation and H_2O removal.

Combining the analyses of Raman and EPR spectroscopies, we observed a paramagnetic superoxo-cobalt species $(Co–O–O)^{2+}$ in the reduced CoAPO-11 under room temperature oxygen adsorption but no similar observation in the reduced CoAPO-5 [29]. The

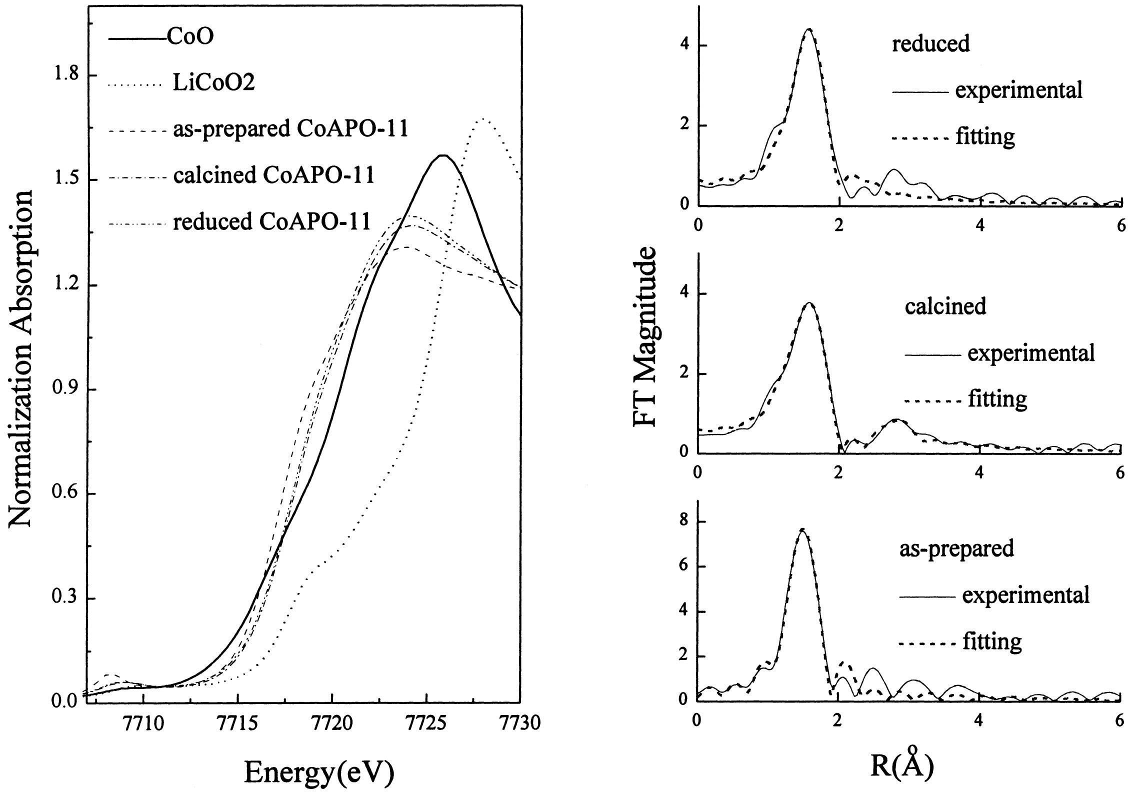

Fig. 1. (a) Normalization Co K-edge XANES spectra. (b) Fourier transforms of $k^3_\chi(k)$ of CoAPO-11.

interaction between O_2 with a Co^{2+} site of reduced CoAPO-11 could be assigned as O_2+Co^{2+}→$Co^{3+}O_2^-$. Such Co^{3+} species may be stabilized by solvent in liquid phase and they may play certain role in the catalytic activity of CoAPO-11 on the oxidation of paraffins and alcohols. It is also known that Co^{2+} species can be oxidized to Co^{3+} by hydrogen peroxide.

For better understanding of the variation of local coordination and oxidation state of Co in CoAPO-11 under redox conditions, the Co K-edge XAS spectra of as-prepared, 550°C (48 h) dry O_2 calcined and 500°C H_2 (4 h) reduced CoAPO-11 samples were collected on the beamline S-5B at 1.5 GeV, Synchrotron Radiation Research Center in Taiwan as shown in Fig. 1. The sample was synthesized, and then treated in a glass U-tube with an attached vacuum valve as reported previously [30]. Before each measurement, the treated sample was packed on an EXAFS sample cell in an argon purged dry bag and sealed with a kapton film. The raw data were processed using the program of UWXAFS 3.0 from University of Washington, Office of Technology Transfer in Seattle. The pre-edge features and edge positions are found to be similar for all CoAPO-11 samples and this indicates that cobalt ions are mainly in oxidation state of 2+. This has been confirmed by X-ray photoelectron spectroscopy (XPS) shown in Fig. 2. The XPS profiles correspond to a monopole charge-transfer process (shake-up) from O 2P to Co 3P and are the characteristic of photoionization of Co^{2+} ions [30]. The energy differences between Co $2P_{1/2}$ and Co $2P_{3/2}$ peaks for as-prepared, calcined and reduced samples are 15.9, 15.6 and 15.8 eV, respectively, they are close to that of Co^{2+} compound (16.0 eV) rather than that Co^{3+} compound (15.0 eV). EXAFS results obtained from analyzing the first coordination sphere around Co are compared with that of CoAPO-18 and CoAPO-5

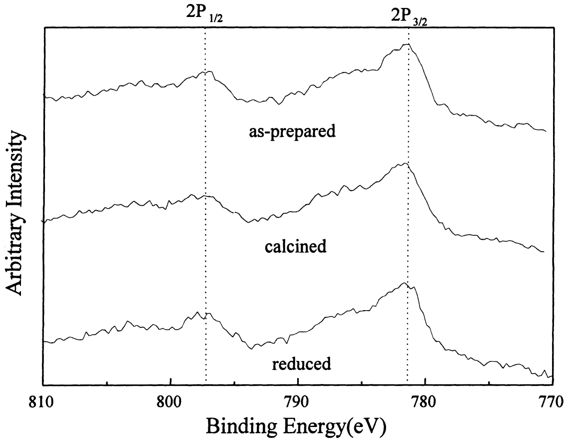

Fig. 2. XPS spectra of CoAPO-11.

measured by Barrett et al. [15] and are summarized in Table 1. The calcination treatment would distort the coordination sphere of Co sites in CoAPO-11 and converted from four identical Co–O distance of 1.95 Å in synthetic form to two and half long Co–O bonds and one short Co–O bond. Upon further reduction, the bond distance of the short Co–O bond returned from 1.90 to 1.96 Å. Nevertheless, both calcined and reduced CoAPO-18 possess three short Co–O bonds and one long Co–O bond. For CoAPO-5, only one type of Co–O bond was observed with bond distances of 1.94, 1.92 and 1.94 Å for as-prepared, calcined and reduced forms, respectively. Barett et al. [15] suggested that the unoxidized Co species in calcined CoAPOs could be involved in the formation of oxygen vacancies that, in turn, were responsible for the low and "unsaturated" coordination number (CN) such as CN=3.6 for calcined CoAPO-5. Consequently, the formation of oxygen vacancy could occur in the reduced form as in the calcined form of CoAPO-11. During redox treatment, water molecules were always formed and could attach themselves to cobalt ions as complexing agents at slightly longer distance. That was not substantiated in the present analysis. The results indicate that the nature of coordination chemistry of CoAPO-11 under redox treatment should be different from that of CoAPO-5 and CoAPO-18. Therefore, as expected, CoAPO-18 exhibits Brønsted acidity only after reduction and not after calcination while CoAPO-11 contains strong Lewis acid sites after calcination and subsequently reduction [22]; furthermore, the medium pore CoAPO-11, unlike the large pore CoAPO-5, seems to be more difficult to be reduced and changes back to the blue color after calcination and is relatively easy to produce O_2^- species with O_2 after reduction [27,30]. It appears that the color change of CoAPOs under redox treatments may also be caused by either the variation of spin states and coordination geometry or the different oxidation state of framework Co.

3. VAPO molecular sieves

3.1. Framework incorporation

Current literature mainly focused on VAPO-5 and whether the isomorphous substitution can be used to describe the incorporation of vanadium in a tetrahedral $AlPO_4$ framework is still debatable. Based on EPR and ^{51}V NMR studies combined with chemical compositional analysis results, Rigutto and van Bekkum observed that V was not leached out from VAPO after catalytic reactions. They proposed that a monomeric vanadyl unit is in either square pyramidal or distorted octahedral coordination of 4+ state for as-prepared sample and of 5+ state for the calcined sample as the main V species in VAPO-5 that occupies an Al site [10]. Montes et al. [31] speculated that, in oxidized VAPO-5, V^{5+} was bonded to four Al sites through O atoms, while in as-prepared and reduced VAPO-5,the vanadyl species (VO^{2+}) neutralized two $\equiv$Al–O^- groups. They further believed, as did Jhung et al. [32], that V^{5+} and/or V^{4+} might be located in a tetrahedral position of $AlPO_4$ framework and would substitute for P^{5+}. Weckhuysen et al. [33] suggested that EPR would only detect the presence of V^{4+} as isolated, oxidized and/or anchored V species, and could not provide unambiguous evidence for isomorphous substitution. Comparing EPR results with IR data, Lohse et al. [34] pointed out that V was not capable of occupying tetrahedral sites as Si and Co in $AlPO_4$ framework, but it could be fixed on the framework by condensation between VO^{2+} ions and hydroxyl groups of $AlPO_4$-44 and -5 matrix. Our previous UV–Vis and Raman measurements detected the existence of V^{5+} with terminal V=O group in the calcined VAPO-5 [12]. Nevertheless, synthetic VAPOs obtained by hydrothermal synthesis in an acid medium

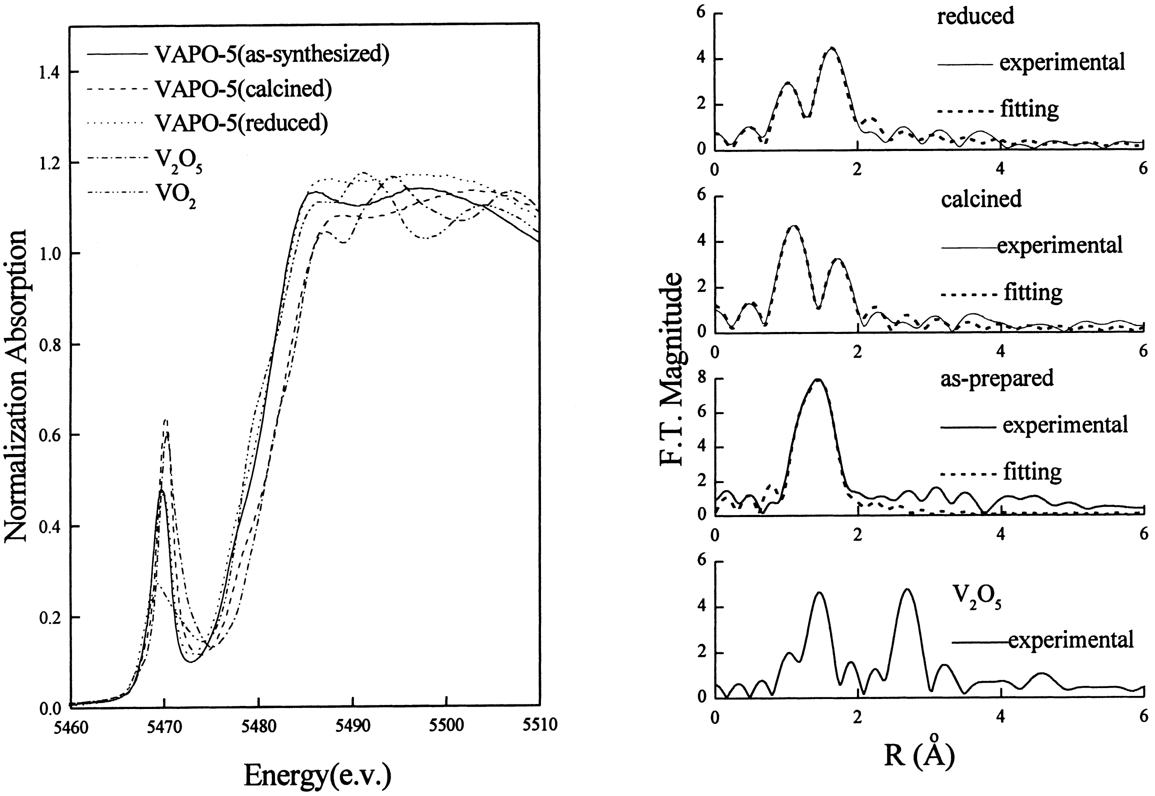

Fig. 3. (a) Normalized V K-edge XANES spectra. (b) Fourier transforms of $k^3_\chi(k)$ of VAPO-5 compared with that of V_2O_5.

exhibit well-dispersed monomeric vanadyl VO^{2+} form, which is independent of the source of vanadium reagents of V_2O_5, $VOSO_4$, etc. and can be readily oxidized to V^{5+} species after calcination treatment. To better understand the coordination chemistry of V species, as-prepared, 500°C (8 h) dry O_2-calcined and 500°C (1 h) H_2 reduced VAPO-5 have been prepared similar to the procedures reported before [12] and were characterized by X-ray absorption. The normalized XANES spectra and their EXAFS Fourier transforms (FTs) of VAPO-5 are compared with those of VO_2 and V_2O_5 as shown in Fig. 3. The refinement of EXAFS data yields a reasonable set of structural parameters given in Table 2. No appreciable peak due to V–V (R=2.7 Å, without phase correction) pairs has been observed in all FTs of VAPO-5. EXAFS/XANES indicates that the V species with a terminal V=O group mainly exist in two V–O-legged complexes on $AlPO_4$-5 framework and they can stay in isolated form after redox treatment.

Table 2
Structural parameters of VAPO-5

Samples		R (Å)	N	σ^2
VAPO-5				
As-prepared	$V–O_1$	1.62	1.2	0.3×10^{-3}
	$V–O_2$	1.99	2.3	5.7×10^{-3}
Calcined	$V–O_1$	1.61	1.0	0.2×10^{-3}
	$V–O_2$	1.68	0.7	0.2×10^{-3}
	$V–O_3$	1.88	2.3	5.8×10^{-3}
Reduced	$V–O_1$	1.66	1.0	0.3×10^{-3}
	$V–O_2$	1.95	1.8	1.3×10^{-3}

3.2. Redox behavior

The coordinations and the oxidation states of V sites in VAPO-5 under redox treatments were investigated by XANES/EXAFS. In the XANES spectra (Fig. 3(a)), we notice the following: (1) The positions and intensities of the pre-edge absorption peak (due to the 1s→3d transition) with the absorption edge of

K-edge of as-prepared and reduced VAPO-5 are very similar and are located at 5469.7 or 5470.0 eV with 5481.7 eV, indicating V sites both for as-prepared and reduced VAPO-5s in the same coordination system and their average oxidation states close to 4+ VO_2 (lower intensity). As a reference, the center of pre-edge peak and the absorption edge of K-edge of VO_2 are 5469.4 (low intensity) and 5478.4 eV. (2) The center of pre-edge absorption peak and the absorption edge of K-edge for calcined VAPO-5 are similar to those for V_2O_5 (5470.3 and 5481.1 eV) and is located at 5470.3 and 5483.2 eV, respectively, but the width of pre-edge peak for calcined VAPO-5 is narrower than that of V_2O_5. This shows that upon calcination, V^{4+} ions are completely oxidized to V^{5+} ions and could exist in a different coordination environment from that of V_2O_5. However, the analysis of EXAFS data reveals that V^{5+} species in a calcined sample are in fourfold coordination with two long V–O bonds and two short V–O bonds, the short V–O distance is symptomatic of a double bond and a terminal oxo group. This type of dioxovanadate units was proposed to take place on anatase TiO_2 or γ-Al_2O_3 supported vanadium oxide [35] and on inorganic cyclo-tetrametra vanadate salt [36]. Furthermore, the refined V–O bond distances of 1.61, 1.68 and 1.88 Å on VAPO-5 are close to those on γ-Al_2O_3 (1.67 and 1.82 Å) and on TiO_2 (1.65 and 1.90 Å). Since no V–V bonds are observed on all the VAPO-5 samples, an indication of the existence as isolated vanadyl units for both V^{4+} and V^{5+} species. On the basis of the results discussed above, the schemes of oxidation and reduction of vanadium sites may be proposed as follows:

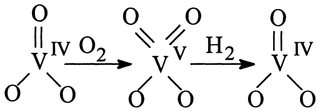

VAPOs were observed to possess catalytic activity on oxidation reactions using either hydrogen peroxide and alkyl hydroperoxides as oxidants in liquid phase or molecular oxygen as the oxidant in gas phase [10,24,37], this is quite similar to V-containing silicate molecular sieves [38,39], such catalytic reactions may involve the redox behavior of framework V^{5+}/V^{4+}. However, part of V were observed to be leached out from the silicate framework after reacting with peroxide [38] and were aggregated into clusters on silicate surface after redox treatment [40]. On the contrary, framework V of VAPOs appear to exist as discrete V species during reaction and redox treatments. This may be caused by either the bonding between vanadyl ions and, perhaps, Al–O groups or the coordination of V atoms in VAPOs under redox treatment. Comparing with V-silicates, $AlPO_4$ tetrahedral framework seems to provide stronger support for the interaction of the vanadyl groups of V^{4+} and V^{5+} than SiO_2 tetrahedral framework.

References

[1] E.M. Flanigen, R.L. Patton, S.T. Wilson, Stud. Surf. Sci. Catal. 37 (1987) 13.
[2] J.C. Vedrine, Stud. Surf. Sci. Catal. 69 (1991) 25.
[3] G. Bellussi, M.S. Rigutto, Surf. Sci. Catal. 85 (1994) 177.
[4] R. Murugavel, H.W. Roesky, Angew. Chem., Int. Ed. Engl. 36 (1997) 477.
[5] R. Szoxtak, Molecular Sieves; Principles of Synthesis and Identification, Van Nostrand Reinhold, New York, 1989.
[6] K.J. Chao, S.P. Sheu, H.S. Sheu, J. Chem. Soc., Faraday Trans. 88 (1992) 2949.
[7] J.M. Bennett, B.K. Marcus, Stud. Surf. Sci. Catal. 37 (1987) 269.
[8] B. Kraushaar-Czarnetzki, W.G. Hoogervorst, W.H.J. Stork, Stud. Surf. Sci. Catal. 84 (1994) 1869.
[9] K.J. Chao, C.N. Wu, H. Chang, L.J. Lee, S.F. Hu, J. Phys. Chem. 101 (1997) 6341.
[10] M.S. Rigutto, H. van Bekkum, J. Mol. Catal. 81 (1993) 77.
[11] R.A. Schoonheydt, R. de Vos, J. Pelgrims, H. Leeman, Stud. Surf. Sci. Catal. 49 (1988) pp. 13, 393.
[12] L.E. Iton, I. Choi, J.A. Desjardins, V.A. Maroni, Zeolites 9 (1989) 535.
[13] A. Montes, M.E. Davis, B. Murray, M. Narayana, J. Phys. Chem. 94 (1990) 6425.
[14] P. Feng, X. Bu, G.D. Stucky, Nature 388 (1997) 735.
[15] P.A. Barrett, G. Sankar, C.R.A. Catlow, J.M. Thomas, J. Phys. Chem. 100 (1996) 8977.
[16] L.J. Leu, K.J. Chao, Proc. Natl. Sci. Counc. ROC (A) 12 (1988) 91.
[17] S.H. Chen, S.P. Sheu, K.J. Chao, J. Chem. Soc., Chem. Commun. (1992) 1504.
[18] L. Canesson, Y. Bondeville, A. Tuel, J. Am. Chem. Soc. (1997).
[19] S. Ernst, L. Puppe, J. Weitkamp, Stud. Surf. Sci. Catal. 49 (1989) 447.
[20] M. Niwa, N. Katada, M. Sawa, Y. Muakami, J. Phys. Chem. 99 (1995) 8812.
[21] M.P.J. Peeters, Ph.D. Thesis, Technische Universiteit Eindhoven, Thesis, Technische Universiteit Eindhoven, Netherland, 1993.

[22] J.M. Thomas, C.N. Greaves, G. Sankar, P.A. Wright, J. Chen, A.J. Dent, L. Marchese, Angew. Chem., Int. Ed. Engl. 33 (1994) 1871.

[23] M.P.J. Peeters, M. Busio, P. Leijten, Appl. Catal. A 118 (1994) 51.

[24] P. Concepción, A. Corma, J.M. López Nieto, J. Pérez-Pariente, Appl. Catal. A 143 (1996) 17.

[25] P.S.E. Dai, R.H. Petty, C.W. Ingram, R. Szostak, Appl. Catal. A 143 (1996) 101.

[26] J.D. Chen, R.A. Sheldon, J. Catal. 153 (1995) 1.

[27] J. Chen, G. Sankar, J.M. Thomas, R. Xu, G.N. Greaves, D. Waller, Chem. Mater. 4 (1992) 1371.

[28] V. Kurshev, L. Kevan, D.J. Parillo, C. Pereira, G.T. Kokotailo, R.J. Gorte, J. Phys. Chem. 98 (1994) 10 160; A.M. Prakach, M. Hartman, L. Kevan, J. Phys. Chem. 101 (1997) 6819.

[29] C.N. Wu, K.J. Chao, H. Chang, L.J. Lee, C. Naccache, J. Chem. Soc., Faraday Trans. 93 (1997) 3551.

[30] T.J. Chuang, C.R. Brundle, D.W. Rice, Surf. Sci. 59 (1976) 413.

[31] C. Montes, M.E. Davis, B. Murray, M. Narayana, J. Phys. Chem. 94 (1990) 6431.

[32] S.H. Jhung, Y.S. Uh, H. Chon, Appl. Catal. 62 (1990) 61.

[33] B.M. Weckhuysen, I.P. Vannijvel, R.A. Schoonheydt, Zeolites 15 (1995) 482.

[34] U. Lohse, A. Brücker, K. Kintscher, B. Parlitz, E. Schreier, J. Chem. Soc., Faraday Trans. 91 (1995) 1173.

[35] J. Haber, A. Kozlowsba, R. Kozlowski, J. Catal. 102 (1986) 52.

[36] P. Roman, Inorg. Chem. 32 (1993) 775.

[37] G. Centi, F. Trifiro, Appl. Catal. A 143 (1996) 3.

[38] S. Gontier, A. Tuel, Microporous Mater. 5 (1995) 161.

[39] T. Sen, V. Ramaswamy, S. Ganapathy, P.R. Rajamohanan, S. Sivasanker, J. Phys. Chem. 100 (1996) 3809.

[40] H. Morey, A. Davidson, H. Eckert, G. Stucky, Chem. Mater. 8 (1996) 486.